PHYSICAL REVIEW E **67**, 060902(R) (2003)

Kinetic pathway of the bilayered-micelle to perforated-lamellae transition

H. Wang,[1,2,*] M. P. Nieh,[2,3] E. K. Hobbie,[2] C. J. Glinka,[2] and J. Katsaras[3]
[1]*Department of Materials Science and Engineering, Michigan Technological University, Michigan 49931, USA*
[2]*National Institute of Standards and Technology, Gaithersburg, Maryland 20899, USA*
[3]*National Research Council, Steacie Institute for Molecular Sciences, Bldg. 459, Stn. 18, Chalk River, Ontario, Canada K0J 1J0*
(Received 6 September 2002; revised manuscript received 1 April 2003; published 30 June 2003)

Using time-resolved small-angle neutron scattering, we have studied the kinetics of the recently observed bilayered-micelle (or so-called ''bicelle'') to perforated-lamellar transition in phospholipid mixtures. The data suggest that phase-ordering occurs via the early-time coalescence of bicelles into stacks of lamellae that then swell. Our measurements on this biomimetic system highlight the ubiquitous role of transient metastable states in the phase ordering of complex fluids.

DOI: 10.1103/PhysRevE.67.060902 PACS number(s): 87.16.Dg, 87.14.Cc, 64.70.Md, 61.12.−q

Lipids are amphiphilic molecules and are one of the principal components of biological membranes forming a selectively permeable barrier between the cell's inner and outer environments. For the most part, lipids are composed of two hydrophobic hydrocarbon chains and a hydrophilic headgroup which can either be charged, as in the case of phosphatidylglycerols, or possess no net charge, as exemplified by the commonly studied phosphatidylcholines. Depending on the nature of their headgroup and fatty acid chains, when dispersed in water, lipid molecules self-assemble into a variety of ordered and disordered phases [1–4]. These mesostructures, many of which are also observed in liquid crystalline [5] and block copolymer melts [6], have spatial symmetry that is intermediate to the short-range positional order of a fluid and the long-range positional and rotational order of a crystalline solid. Although a great deal of work has been done to quantify the rich phase behavior and morphology of such surfactant systems, phase transition kinetics following a quench have, for the most part, received limited attention [7–9]. Such nonequilibrium studies are of fundamental importance, as they illuminate the kinetic pathways that complex fluids use to relax to inherently more stable structures [7–10].

In recent years, bilayered micelles (Fig. 1), or so-called ''bicelles'' composed of short-tail and long-tail phospholipids, have received considerable attention as potentially important magnetically alignable substrates for solid-state nuclear magnetic resonance and neutron scattering studies of membrane-associated peptides and proteins [11–15]. Despite this widespread interest, there has been much debate regarding the nature of the structural phases formed by such mixtures. Recently, small-angle neutron scattering (SANS) studies carried out by Nieh *et al.* [14,15] on mixtures of long-chain [e.g., the zwitterionic lipid dimyristoyl phosphatidylcholine (DMPC) and the negatively charged lipid dimyristoyl phophatidylglycerol (DMPG)] and short-chain [e.g., dihexanoyl phosphatidylcholine (DHPC)] phospholipids, demonstrated that in addition to vesicles, the lipid mixture formed bilayered micelles and ordered stacks of perforated lamellae. The phase diagram and the corresponding microstructures are schematically illustrated in Fig. 1. At high lipid concentration ($c_l > 0.025$ g/ml), the bicellar phase forms at lower temperatures ($T < 23\,^{\circ}$C) with DHPC presumably decorating the rim of the micelle, whereas for the perforated lamellar phase at high temperatures, DHPC molecules line the holes perforating the lamellae [14]. This observation was is in contrast to the general view that smectically ordered bilayered micelles populate the high-T phase [12,16]. The gray regions in Fig. 1 depict areas of two-phase coexistence.

The nature of the newly found bilayered micelle-to-lamellar transition [14,15] is intricate. Initiated by hydrocarbon-chain melting and increased lipid mobility within the bilayers, it is otherwise analogous to the isotropic-to-smectic transition in liquid crystals and the order-disorder transition in block copolymers. It can be characterized as a global first-order transition that is kinetically limited by a local first-order transition at the molecular scale. In this study, we investigate the phase-ordering kinetics of the bilayered micelle-to-lamellar transition using time-resolved SANS. Smectic ordering is observed to occur via a two-step process, and we extract both a ''local'' time scale characterizing the coalescence of bicelles into stacks of lamellae and a ''global'' time scale characterizing the subsequent swelling of those stacks. The measurements highlight the important

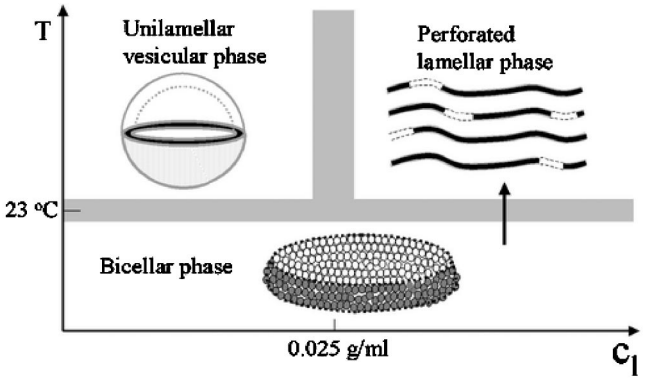

FIG. 1. Schematic of the phase diagram determined by Nieh *et al.* [14] showing the of vesicular, bicellar, and lamellar phases. The arrow indicates the lipid concentration at which the temperature studies were carried out.

*Corresponding author. Email address: wangh@mtu.edu

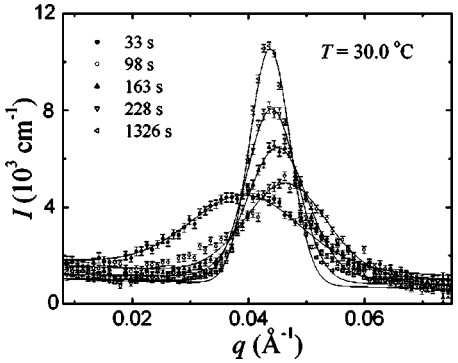

FIG. 2. The evolution, as a function of time, of a typical SANS spectrum following a quench from 0 to 30.0 °C. The solid curves are Gaussian fits. The characteristic length scale of the lipid mixture is given by the peak position.

role of transient metastable states in the phase ordering of complex fluids.

DMPC (zwitterionic, two 14:0 hydrocarbon chains), DHPC (zwitterionic, two 6:0 hydrocarbon chains), and DMPG (negatively charged, two 14:0 hydrocarbon chains) were purchased from Avanti Polar Lipids (Alabaster, AL) and used without further purification [17]. The negatively charged lipid, DMPG, was used to stabilize the lamellar phase and prevent phase separation of the short-chain DHPC lipid from DMPC. Samples of DMPC:DHPC:DMPG in a molar ratio of 5:1:0.25 were mixed in 80% D_2O by weight. The mixtures were temperature cycled and agitated until homogeneous. The samples were then transferred to a copper sample cell with a path length of 1.5 mm and sealed.

Time-resolved SANS measurements were performed using the 8m SANS instrument at the NIST Center for Neutron Research. Incident neutrons of wavelength $\lambda = 10$ Å$(\Delta\lambda/\lambda = 0.15)$ yielded a range of scattering wave vector, $0.008\ \text{Å}^{-1} < q < 0.08\ \text{Å}^{-1}$. The resolution of the SANS measurement is, for the most part, dictated by the neutron wavelength dispersion and is adequate to reveal the supramolecular organization of lipids in the system studied. In quenching the mixtures, samples were rapidly transferred from ice water (0 °C) to a sample stage preequilibrated between $T = 22.0$ and $45.0(\pm 0.2)$ °C. For the deepest quenches, the sample reached thermal equilibrium in under 40 s, which was independently measured. The two-dimensional (2D) intensity patterns were recorded for a 15 s period at intervals of 55 s and are consistent with a multidomain or "powder" morphology.

Typical time-resolved spectra, corresponding to the nonequilibrium structure factor of the ordering fluid, are shown in Fig. 2 for a quench at 30.0 °C. Time t is chosen as the mean of the measurement interval. The peak position q_m initially increases up to $t = 98$ s and from then on continually decreases, indicative of structural changes. The initial low-T phase is made up of disordered bicelles [14], while the formation of the high-T perforated lamellar phase is due to bicelles coalescing as a result of increased hydrocarbon chain disorder and increased lipid mobility. The perforated bilayers then further associate into multilamellar stacks. The value of q_m corresponds to the characteristic length $L_m = 2\pi/q_m$. At

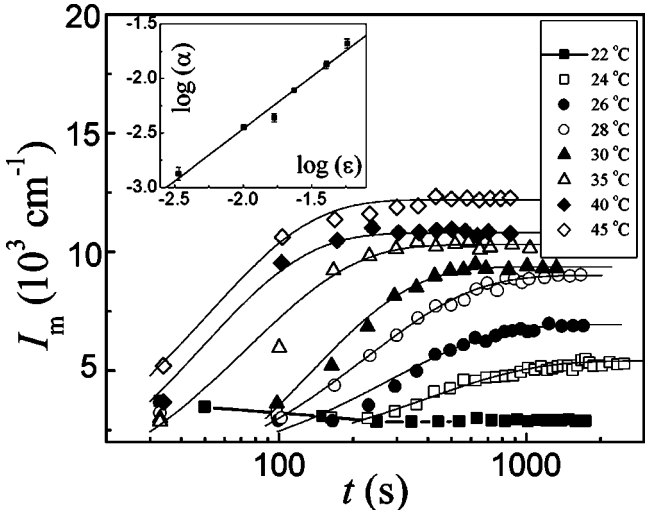

FIG. 3. The evolution of $I_m(t)$ at various temperatures T where the inset shows the relaxation rate α as a function of quench depth $\epsilon = (T - T_c)/T_c$.

low T, L_m is approximately the mean bicelle separation and at high T, the mean separation between the lamellae. Moreover, as the peak intensity I_m increases, the peak full width at half maximum σ_q decreases. In the case of the perforated lamellar phase the broadening of the scattering peak can be attributed to a number of factors, such as limited number of lamellae in a stack, bilayer fluctuations, defects in bilayers (e.g., perforations) and at domain boundaries, and a broad distribution of lamellar spacings as a result of kinetically trapped stacks. In addition, we focus on the evolution of peaks corresponding to the average bicelle separation and the first-order diffraction peak of the lamellar stack, respectively. Coexistence of the two structures, as well as convolution with the instrumental resolution, leads to a primary scattering feature that we approximate by a Gaussian distribution, $I(q) = I_m \exp[-(q - q_m)^2/2\sigma_q^2]$. The solid curves in Fig. 2 are fits with a constant background arising from homogeneous features and incoherent scattering.

The extent and quality of the lamellar stacking are measured by the peak intensity I_m and peak width σ_q. Figures 3 and 4 show the evolution, for various quenches, of I_m and σ_q, respectively. At 22.0 °C (still within the disordered bicellar phase), I_m and σ_q are similar to those at 0 °C. However, for quenches into the ordered lamellar region of the phase diagram [14], I_m varies inversely with σ_q, as can be seen by comparing Figs. 3 and 4. Following a shallow quench ($T < 27$ °C), I_m remains relatively constant for a short period of time before growing to a plateau, while σ_q remains initially constant and then decays to a plateau at later t. The square of the final value $\sigma_{q,f}^2$ as a function of T^{-1} (inset to Fig. 4) exhibits a sharp increase at $T_c = 23$ °C, the transition temperature.

The first-order phase transitions typically occur via the nucleation and growth of a final stable phase from an initial metastable phase. The picture can be complicated by the presence of local minima in the free energy in which the system resides temporarily or becomes kinetically trapped. If the initial state of the fluid is not far removed from the final

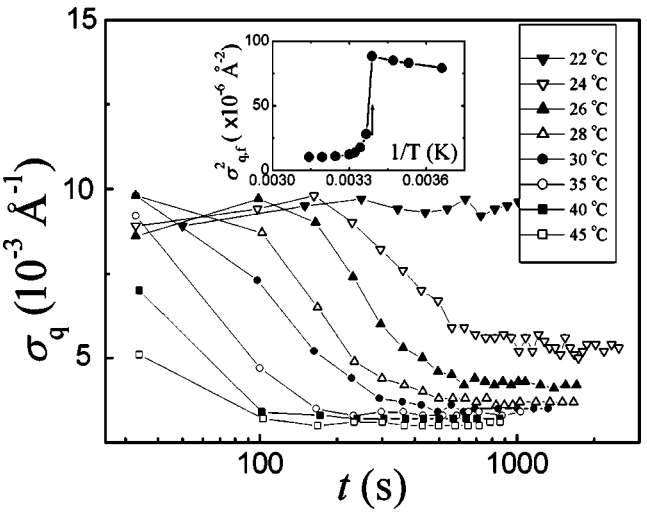

FIG. 4. The evolution of $\sigma_q(t)$ for various quenches. The inset shows the square of the final plateau value as a function of $1/T$, with the transition indicated by an arrow.

equilibrium state (within the parameter space being measured), then it is reasonable to model the ordering process as a simple exponential relaxation, with the decay time arising from a combination of energetic and kinetic influences. We have thus fitted the late-time growth exhibited by $I_m(t)$ to the exponential relaxation $I_m(t)=I_m(\infty)[1-\exp(-\alpha t)]$, where the fits in Fig. 3 assume an initial period of dormancy that coincides with the rapid coalescence of bicelles. The effective relaxation rate α varies linearly with quench depth, defined as $\epsilon=(T-T_c)/T_c$ (inset to Fig. 3), consistent with a global transition that is weakly first order.

The physical significance of the initial period of coalescence is better demonstrated in Fig. 5, which shows $L_m(t)$ for several quenches. At shallow quenches, ($T<27\,^\circ$C), L_m decreases monotonically from around 180 Å to a constant

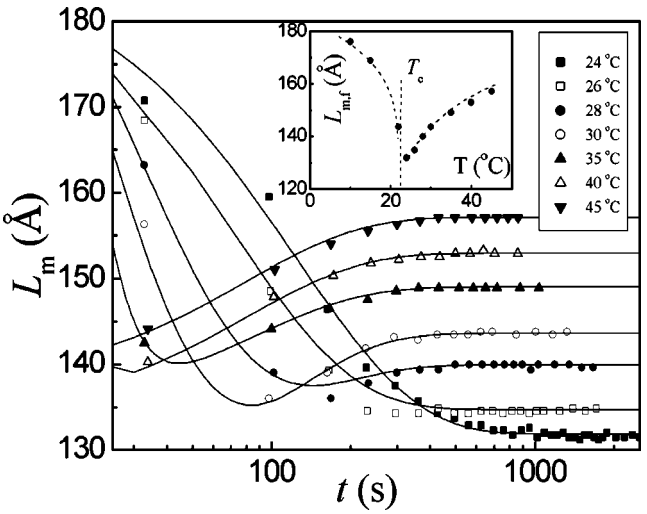

FIG. 5. The evolution of $L_m(t)$ for different quench depths, where the curves represent fits described in the text. The inset shows the T-dependent, steady state $L_{m,f}$, where the transition is indicated by a dashed line. The dashed curves are guides to the eye.

value. For $T>27\,^\circ$C, L_m decreases initially to a minimum, and then increases to a plateau. The initial decrease occurs at an increasing rate as T increases. Above 35.0 °C, the initial process is so rapid that L_m reaches a minimum and begins to increase monotonically before the first measurement interval is complete. The inset to Fig. 5 shows the characteristic length of the system in the steady state $L_{m,f}(T)$ for both bicelle and lamellar phases. $L_{m,f}(T)$ has a minimum at T_c, and increases away from the transition, resulting in an inverted "λ" shape. In the lamellar phase, the plateau might reflect a kinetically arrested multidomain structure. With increased lipid mobility at larger values of ϵ, the lamellar domains can grow larger before the energy barrier associated with further swelling becomes too large to be overcome within the time scale in question (tens of minutes). Thus, at higher Ts the volume fraction of interdomain regions, where the excess water molecules reside, is smaller; stacks incorporate more water, resulting in a larger repeat spacing. On much longer time scales (hours to days), the smectic domains slowly grow to macroscopic dimensions that are easily resolved using polarized microscopy.

For a phenomenological model of the kinetics, we assume that the average characteristic length measured by SANS is $L_m(t)\approx L_{bi}\phi_{bi}+L_{lam}\phi_{lam}$, where L_{bi} and L_{lam} are the bicelle and lamellar length scales, respectively, and $\phi_{bi}(t)\approx e^{-Mt}$ and $\phi_{lam}(t)\approx 1-\phi_{bi}(t)$ are the volume fractions of the bicellar and lamellar phases, respectively. The bicellar coalescence rate M is limited by lipid mobility. We assume the system is under steady state conditions when the lamellae cease to swell. This complex behavior can be modeled asymptotically as $L_{lam}(t)=L_0+(L^f_{lam}-L_0)(1-e^{-t/\tau})$, where L_0 and L^f_{lam} are the initial and final lamellar periodicity, respectively. The time constant τ characterizes the rate of lamellar swelling. Thus, the overall time dependence of the measured characteristic length of the system can be written as

$$L_m(t)=L_{bi}e^{-Mt}+L_{lam}(t)(1-e^{-Mt}). \tag{1}$$

Equation (1) contains two time scales, $1/M$ and τ. The data in Fig. 5 were fitted using Eq. (1) and measured values for L^f_{lam} and L_{bi} (inset to Fig. 5). The resultant fit yielded $\tau\approx 80$ s and $L_0\approx 135$ Å. τ and L_0 are both independent of T, while M, the only adjustable parameter, is T dependent. The solid lines represent the best fit to the data (Fig. 5). From the T dependence of M, which varies from $1/M\approx 137$ s for the shallowest quench to $1/M\approx 0.36$ s for the deepest quench, a fit via $M(T)=k_1e^{k_2\epsilon}$ gives constants k_1 and k_2 of $(5.5\pm 0.2)\times 10^{-3}$ s^{-1} and 84 ± 2, respectively, suggesting that with increased quench depth, local chain melting speeds up considerably. Due to limited data and finite resolution at early times (up to 100 s), M is approximate for deep quenches. The assumption that τ is independent of quench depth, and hence, M is unrealistic as more than a zeroth-order approximation, particularly since the "swelling" we describe here may be limited at the molecular scale by chain mobility and at the macroscale via the degree of defect pinning of the final steady state.

Kinetic models of the isotropic-smectic transition have focused on the nucleation of smectic droplets near a fluctuation-induced first-order phase transition [18–20]. As a starting point, such models employ the phenomenological free-energy of Brazovskii [21]. Recent observations of entropic isotropic-smectic transitions in rigid-rod suspensions [22], however, suggest that ordering may be initiated by the nucleation of tactoidal nematic droplets, with smectic layers then nucleating off of these metastable objects. Although more measurements are needed to further clarify the nature of the transient states observed here, it seems plausible that an analogous scenario might apply to the bicelle aggregates in question, as one can intuitively envision going from a disordered arrangement to a lamellar arrangement via an intermediate discotic nematic. Metastable intermediate structures were also observed in recent studies of the micelle-to-vesicle transition in surfactant mixtures following a shear [7] or concentration quench [8,9]. A somewhat similar multistep ordering was also observed in the depletion-driven crystallization exhibited by binary colloidal mixtures [23]. The late time swelling of the lamellar spacing may be influenced by grain boundary pinning as a consequence of topological defects [24].

In summary, our data suggest a two-step ordering process by which bilayered micelles coalesce into perforated multibilayer stacks, which then swell into perforated extended lamellae. This scenario suggests that an intermediate, metastable bicelle-aggregate phase might play an important role in the kinetic pathway of the transition. Intermediate metastable states may in fact be ubiquitous in the kinetics of phase transitions [7–10]. We thus hope that the present observations offer further insight into the nature of these nonequilibrium phenomena, particularly in the area of biomimetic systems whose functionality is highly dependent on the stability of complex phases.

[1] J.N. Israelachvili, *Physics of Amphiphiles: Micelles, Vesicles and Microemulsions* (North-Holland, New York, 1985).
[2] G.S. Smith, E.B. Sirota, C.R. Safinya, and N.A. Clark, Phys. Rev. Lett. **60**, 813 (1988).
[3] V.A. Raghunathan and J. Katsaras, Phys. Rev. Lett. **74**, 4456 (1995).
[4] T.C. Lubensky and F.C. MacKintosh, Phys. Rev. Lett. **71**, 1565 (1993).
[5] P.G. de Gennes and J. Prost, *The Physics of Liquid Crystals* 2nd ed. (Clarendon Press, Oxford, 1993).
[6] M.A. Hillmyer, F.S. Bates, K. Almdahl, K. Mortensen, A.J. Ryan, and J. Fairclough, Science **271**, 976 (1996).
[7] S. Schmölzer, D. Gräbner, M. Gradzielski, and T. Narayanan, Phys. Rev. Lett. **88**, 258301 (2002).
[8] S.U. Egelhaaf and P. Schurtenberger, Phys. Rev. Lett. **82**, 2804 (1999).
[9] J. Leng, S.U. Egelhaaf, and M.E. Cates, Europhys. Lett. **59**, 311 (2002).
[10] V.J. Anderson and H.N.W. Lekkerker, Nature (London) **416**, 811 (2002).
[11] J. Katsaras, R.L. Donaberger, I.P. Swainson, D.C. Tennant, Z. Tun, R.R. Vold, and R.S. Prosser, Phys. Rev. Lett. **78**, 899 (1997).
[12] C.R. Sanders and J.P. Schwonek, Biochemistry **31**, 8898 (1992).
[13] B.J. Hare, J.H. Prestegard, and D.M. Engleman, Biophys. J. **69**, 1891 (1995).
[14] M.P. Nieh, C.J. Glinka, S. Kruger, R.S. Prosser, and J. Katsaras, Langmuir **17**, 2629 (2001).
[15] M.P. Nieh, C.J. Glinka, S. Kruger, R.S. Prosser, and J. Katsaras, Biophys. J. **82**, 2487 (2002).
[16] R.R. Vold and R.S. Prosser, J. Magn. Reson., Ser. B **113**, 267 (1996).
[17] The references to commercial equipment or materials do no imply recommendation or endorsement by NIST.
[18] G.H. Fredrickson and K. Binder, J. Chem. Phys. **91**, 7265 (1989).
[19] P.C. Hohenberg and J.B. Swift, Phys. Rev. E **52**, 1828 (1995).
[20] N.A. Gross, M. Ignatiev, and B. Chakraborty, Phys. Rev. E **62**, 6116 (2000).
[21] S.A. Brazovskii, Sov. Phys. JETP **41**, 85 (1975).
[22] Z. Dogic and S. Fraden, Philos. Trans. R Soc. London, Ser. A **359**, 997 (2001).
[23] E.K. Hobbie, Phys. Rev. Lett. **81**, 3996 (1998).
[24] D. Boyer and J. Vinals, Phys. Rev. E **65**, 046119 (2002).